LONGITUDINAL SPIN STRUCTURE OF THE NUCLEON: DATA AND PERSPECTIVE ON THE ELECTRON–ION COLLIDER*

Maria Zurek

Argonne National Laboratory, Lemont, Illinois 60439

Received 23 April 2023, accepted 24 April 2023, published online 6 September 2023

Spin is a unique probe to unravel the internal structure and QCD dynamics of nucleons. The exploration of the spin structure of nucleons is based on the complementarity of lepton scattering processes and purely hadronic probes. One of the main questions that physicists have been trying to address in spin experiments involving different interactions and probes is: how does the spin of the nucleon originate from its quark, anti-quark, and gluon constituents and their dynamics? These proceedings provide a snapshot of selected recent experimental results probing the longitudinal spin structure of nucleons utilizing both lepton scattering processes and hadron–hadron interactions, such as Deep Inelastic Scattering experiments in Jefferson Lab, CERN, and DESY, as well as the RHIC spin program with pp collisions. The future opportunities at the Electron–Ion Collider are also briefly described.

DOI:10.5506/APhysPolBSupp.16.7-A3

1. Introduction

The distribution of the spin of the proton among its quark, anti-quark, and gluon constituents has been a fundamental challenge for strong interaction physics. Decades of polarized Deep Inelastic Scattering experiments at SLAC, CERN, DESY, and JLab have studied the polarized DIS cross section that encodes information about the helicity structure of quarks inside the proton [1–17]. These experiments have shown that only about 25–30% of the proton's spin comes from the spins of quarks and anti-quarks [18–29]. The rest must originate from the spins of the gluons and the orbital angular momenta of the quarks and gluons which can be expressed, *e.g.*, using the Jaffe–Manohar spin sum rule

* Presented at the 29$^{\text{th}}$ Cracow Epiphany Conference on *Physics at the Electron–Ion Collider and Future Facilities*, Cracow, Poland, 16–19 January, 2023.

$$\tfrac{1}{2} = \tfrac{1}{2}\sum_{q} \Delta q + \Delta G + L_q + L_g\,, \tag{1}$$

where Δq is the spin carried by each quark flavor, ΔG is the spin carried by the gluons, L_q is the quark orbital angular momentum, and L_g is the gluon orbital angular momentum. The sum runs over all quark flavors in the proton. This has motivated extensive research to understand the longitudinal spin structure of the proton. Semi-inclusive polarized DIS (SIDIS) experiments [3, 30–36] and measurements of polarized hadroproduction of W-bosons at RHIC [37–42] have shed light on the quark and anti-quark spin contributions by flavor and have revealed an asymmetry in the polarized light quark sea [42, 43]. In addition to these experiments, measurements of the spin-dependent rates of production of jets [44–50], di-jets [48–52], π^0s and charged pions [53–61], and direct photons [62] produced in polarized pp collisions at RHIC provide evidence for positive gluon polarization with a strong constraint from the jet data at a center-of-mass energy of $\sqrt{s} = 200$ GeV [18, 20]. Perturbative QCD analyses [18–20, 63] of the world data at next-to-leading order (NLO) precision suggest that gluon spins could contribute $\simeq 40\%$ to the spin of the proton for gluon fractional momenta $x > 0.05$ at a scale of $Q^2 = 10$ GeV^2.

In this paper, an overview of selected recent experimental results on the longitudinal spin structure of the proton and discussion of the prospects for future measurements at the upcoming Electron–Ion Collider (EIC) are provided. The EIC is expected to provide unprecedented precision measurements of the longitudinal spin structure of the proton.

2. Selected results

This section includes a brief description of recent experimental results on the longitudinal spin structure of nucleons including data sensitive to the gluon helicity, as well as valence and quark-sea asymmetries.

2.1. Gluon helicity

The Solenoidal Tracker at Relativistic Heavy Ion Collider (STAR) and Pioneering High Energy Nuclear Interaction eXperiment (PHENIX) at RHIC address the fundamental question about the origin of the proton spin using collisions of high-energy polarized protons. Since gluon–gluon and gluon–quark scatterings dominate jet production at $\sqrt{s} = 200$ GeV and $\sqrt{s} = 510$ GeV at STAR, measurements of the double-spin asymmetries, $A_{\rm LL}$, of inclusive jet and dijet production in longitudinally polarized proton collisions provide access to the gluon spin contribution to the proton spin. Results for dijet production provide better determination of the functional form of

$\Delta g(x)$, compared to inclusive observables, due to better constraints on the underlying kinematics [19]. Moreover, direct photons, measured recently at PHENIX, are produced from the initial partonic hard scattering and do not interact via the strong force. Therefore, the direct photon $A_{\rm LL}$ measurement presented in the right panel of Fig. 1 provides clean and direct access to the gluons in the polarized proton.

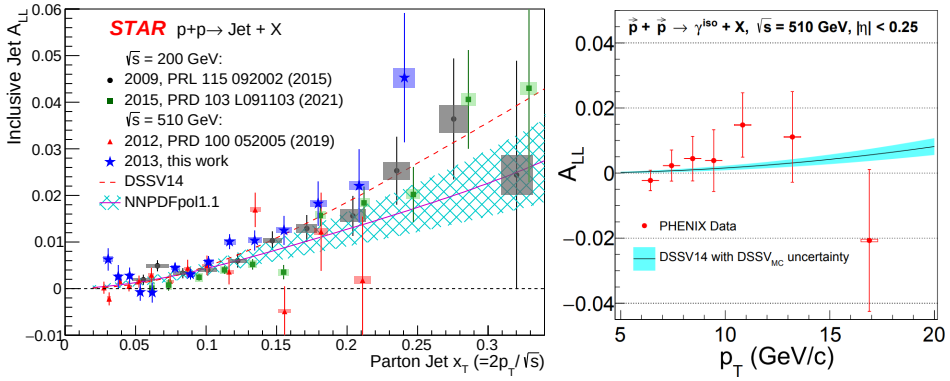

Fig. 1. (Color online) Left: Recent STAR results on inclusive jet $A_{\rm LL}$ *versus* $x_{\rm T}$ at $\sqrt{s} = 200$ GeV [47, 49] and 510 GeV [48, 50] at mid-rapidity from data collected in years 2009–2015, and evaluations from DSSV14 [18] and NNPDFpol1.1 [20] global analyses. The vertical lines are statistical uncertainties. The boxes show the size of the estimated systematic uncertainties. Source: [50]. Right: PHENIX double-helicity asymmetry $A_{\rm LL}$ *vs.* $p_{\rm T}$ for isolated direct-photon production in polarized pp collisions at $\sqrt{s} = 510$ GeV at midrapidity [62]. DSSV14 calculation is plotted as the black curve with the 1σ uncertainty band marked in light blue/gray.

Recent STAR results [48–50] and preliminary results [64–66] on longitudinal double-spin asymmetries of inclusive jet and dijet production at center-of-mass energies of 200 GeV and 510 GeV at mid- and intermediate rapidity complement and improve the precision of previous STAR measurements. The left panel of Fig. 1 shows recent STAR results on inclusive jet $A_{\rm LL}$ *versus* $x_{\rm T} = 2p_{\rm T}/\sqrt{s}$ at $\sqrt{s} = 200$ GeV and 510 GeV at mid-rapidity from data collected in years 2009–2015, and evaluations from the DSSV14 [18] and NNPDFpol1.1 [20] global analyses. The overall impact of the recent jet and dijet [48–50, 52, 65], pion [59, 61], and W [67, 68] data on the x-dependence of the gluon helicity distribution at $Q^2 = 10$ GeV^2 based on the global fit by the DSSV group is presented in Fig. 2. The truncated moment of the gluon helicity from the new preliminary DSSV evaluations [69] at $Q^2 = 10$ GeV^2 integrated with the range $x \in (0.001, 0.05)$ is 0.173(156) and in the range $x \in (0.05, 1)$ is 0.218(27) (at 68% C.L.). The truncated moment of the gluon helicity integrated from $x = 0.0071$ to 1 at $Q^2 = 10$ GeV^2 from the recent

JAM global QCD analysis [63] including a subset of RHIC data, *i.e.*, STAR inclusive jet results, and assuming the SU(3) flavor symmetry and PDF positivity is 0.39(9). RHIC concluded data taking with longitudinally polarized protons in 2015, and the results are expected to provide the most precise insights on ΔG until the EIC data become available.

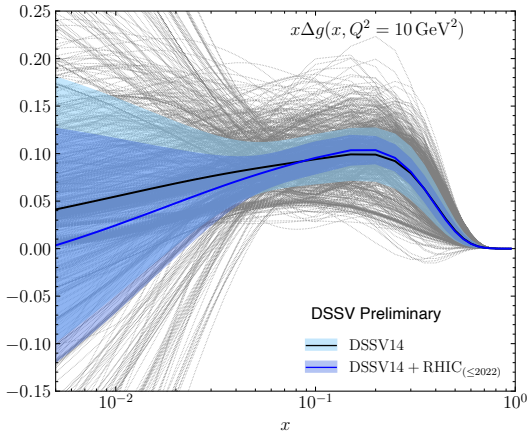

Fig. 2. (Color online) The impact of the recent jet and dijet [48–50, 52, 65], pion [59, 61], and W [39, 40, 42] data on the x-dependence of the gluon helicity distribution at $Q^2 = 10$ GeV^2 based on the global fit by the DSSV group. The black curve with the 1σ uncertainty light blue band illustrates the DSSV14 results [18], while the blue curve with 1σ uncertainty band in dark blue shows the preliminary results after the inclusion of the new data from [69].

2.2. Valence and sea-quark helicities

2.2.1. Legacy SIDIS data

The quark helicities Δq in the valence region have been thoroughly investigated in (SI)DIS with longitudinally polarized protons. Figure 3 presents an example of extracted helicity distributions for valence quarks based on a comprehensive collection of results on longitudinal double-spin asymmetries from SIDIS at HERMES [36] measured with electron and positron beams and proton and deuteron targets. The red dots indicate the results obtained through direct extraction from the pion charge-difference asymmetries, $A_1^{\pi^+ - \pi^-}$, assuming leading-order, leading-twist QCD, charge-conjugation symmetry, and isospin symmetry in fragmentation functions to ensure a clean factorization process, allowing fragmentation without any memory of the target configuration. Alongside these results, the figure displays the same quantities computed using inclusive, A_1, and semi-inclusive asymmetries for the production of negative and positive pions, $A_1^{\pi^{+/-}}$,

through the HERMES purity extraction method [32], which involves the conditional probability of a hadron originating from a struck quark of flavor q, and depends on a fragmentation model.

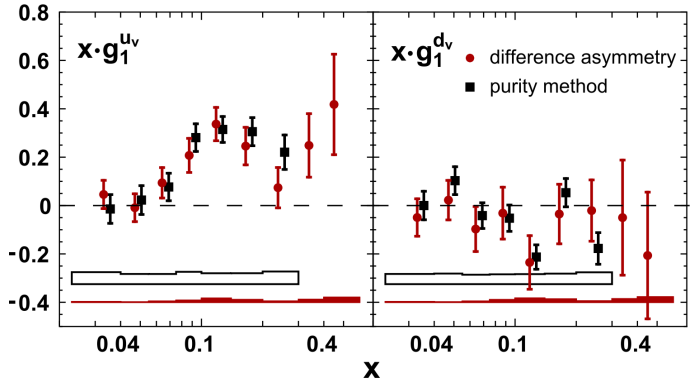

Fig. 3. (color online) The plot compares helicity distributions of valence quarks from the HERMES SIDIS data on pion charge-difference asymmetries [36] with purity extraction [32]. Error bars represent statistical uncertainties, while filled (open) bands show systematic uncertainties from the difference-asymmetry (purity) extraction. Source: [36].

2.2.2. High-x data from Jefferson Lab

Nucleon spin structure in the far valence domain has been also recently studied at Jefferson Lab. For example, the Hall C E12-06-110 experiment with polarized ^{3}He target aims at studying the virtual-photon–nucleon asymmetry A_1 for neutron in the large x region $0.3 < x < 0.77$ and $3 < Q^2 < 10$ GeV^2 [70]. The experiment will provide first precision data in the valence quark region above $x > 0.61$. Furthermore, when this data is combined with the existing world proton data and the projected proton data from CLAS12 [71], it will result in precise determination of the ratios of polarized-to-unpolarized PDFs, namely $\Delta u/u$ and $\Delta d/d$. These outcomes will serve to test a variety of predictions for the behavior of the asymmetry and PDF ratios at $x \to 1$, such as those from the relativistic constituent quark model, leading-order perturbative QCD, and the latest pQCD calculations that incorporate quark orbital angular momentum [72, 73]. Since in the high-x region sea effects are negligible, these experiments will shed light on how much of a role the orbital angular momentum of quarks L_q plays in forming the nucleon spin and to what extent are valence quark spins aligned with the nucleon spin.

In the left panel of Fig. 4, the collected world data on A_1 for the neutron [74–79] using a polarized ^{3}He target is presented alongside predictions from various models such as the relativistic constituent quark model [80], statistical models [26, 81], Nambu–Jona-Lasinio model [82], and two Dyson–Schwinger-equations-based approaches (where the dressed-quark propagator that is momentum-dependent and -independent, respectively, is used in constructing the Faddeev equation) [83]. The pQCD model marked with a blue dashed line assumes the absence of quark orbital angular momentum [84], while the one marked with a pink dotted line explicitly allows for it [85]. The right panel of Fig. 4 shows the preliminary results of the asymmetry A_1 for ^{3}He with statistical uncertainties only. The preliminary results do not include radiative corrections and nuclear corrections to extract the neutron asymmetry from the measured asymmetry on the nuclear target [72, 73].

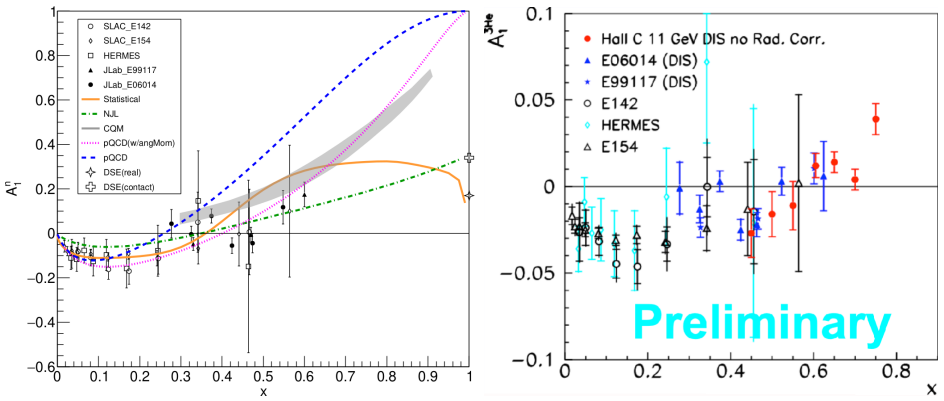

Fig. 4. (Color online) Left: Comparison of current world data on A_1 for neutrons measured using a polarized ^{3}He target with predictions from different models, including the relativistic constituent quark model, statistical and NJL models, and two DSE-based approaches as well as two pQCD models with and without orbital angular momentum (see the text). Right: Preliminary results for the asymmetry A_1 for ^{3}He with statistical uncertainties only. Note that the preliminary results do not include radiative corrections and nuclear corrections. Source: [72, 73].

2.2.3. Quark-sea helicities from RHIC

Quark helicities in the quark-sea region have been studied in proton–proton collisions. The STAR and PHENIX collaborations have concluded measurements of the parity-violating spin asymmetry in weak boson production from collisions with a longitudinally polarized proton beam [37–42] in 510 GeV proton–proton collisions at RHIC. W^+ bosons are mainly produced from u quarks and $\bar{d}$ anti-quarks, while W^- bosons are produced

from d quarks and $\bar{u}$ anti-quarks. Measurements of the longitudinal single-spin asymmetry, A_{L}, for the decay positrons provide information on the u quark and $\bar{d}$ helicities, while the decay electrons provide information on the d and $\bar{u}$ helicities. Together, these measurements enable the flavor-sensitive determination of light quark and anti-quark polarizations in the proton.

The data, shown in the left panel of Fig. 5, are the final results from STAR and PHENIX on this topic that combine all the published data obtained in 2011, 2012, and 2013. The STAR 2013 data [68] were used in the reweighting procedure with the publicly available NNPDFpol1.1 PDFs [20]. The results from this reweighting, taking into account the total uncertainties of the STAR 2013 data and their correlations, are shown in the right panel of Fig. 5 as blue (dark gray) hatched bands. The NNPDFpol1.1 uncertainties are shown as green (light gray) bands for comparison. As seen from the plot, the data have now reached a level of precision that makes it possible, for the first time, to conclude that there is a clear asymmetry between the helicity distribution of $\bar{u}$ and $\bar{d}$, and that it has the opposite sign from the $\bar{d}/\bar{u}$ flavor asymmetry in the unpolarized sea.

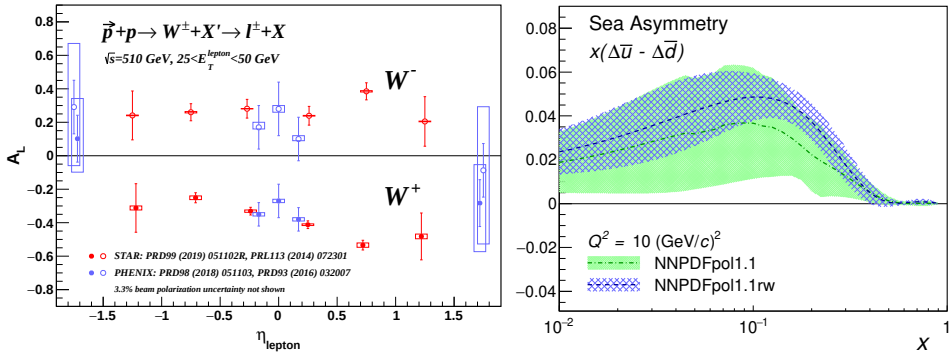

Fig. 5. (Color online) Left: Longitudinal single-spin asymmetries, A_{L}, for W production as a function of the lepton pseudorapidity, η_{lepton}, for the combined STAR and PHENIX data samples [39–42]. Right: The difference of $\bar{u}$ and $\bar{d}$ polarizations as a function of x at a scale of $Q^2 = 10$ GeV^2 before and after NNPDFpol1.1 [20] reweighting with STAR 2013 W A_{L} [68]. The green (light gray) band shows the NNPDFpol1.1 results [20] and the blue (dark gray) hatched band shows the corresponding distribution after the STAR 2013 W data are included by reweighting.

3. Perspectives from the Electron–Ion Collider

The EIC, being the first polarized lepton–proton/nucleus collider, will venture into unexplored areas in spin physics utilizing deep inelastic scattering as a probe of the internal structure of nucleons and nuclei. Apart

from probing the quark sector, the EIC's broad range of Q^2 will allow for the investigation of the scaling violations in the g_1 structure function, which will provide substantial constraints on the gluon helicity down to momentum fractions of about $x = 10^{-4}$. The comparison of the $x - Q^2$ coverage of the EIC at two different center-of-mass energies with polarized ep experiments conducted at CERN, DESY, Jefferson Lab, and SLAC, as well as pp experiments at RHIC is presented in the left panel of Fig. 6. The impact of the projected EIC pseudodata with a total luminosity of 10 fb^{-1} on the gluon helicity is presented in the right panel of Fig. 6. The pseudodata at the center-of-mass energy $\sqrt{s} = 45$ GeV have been included in a new global fit by the DSSV group with extended flexibility of the helicity parametrization. The further impact of the $\sqrt{s} = 140$ GeV pseudodata has been evaluated by reweighting the DSSV14 evaluation with the $\sqrt{s} = 45$ GeV pseudodata included. The uncertainty on the gluon helicity is significantly reduced relative to the DSSV14 baseline [19, 86]. In addition to golden channel g_1 structure function measurements, the EIC will also give us access to higher-order processes such as photon–gluon fusion that will provide direct access to the gluon and serve as an important cross-check to the inclusive result. These probes include the longitudinal double-spin asymmetries for dijets or heavy quarks (see, *e.g.*, [87]).

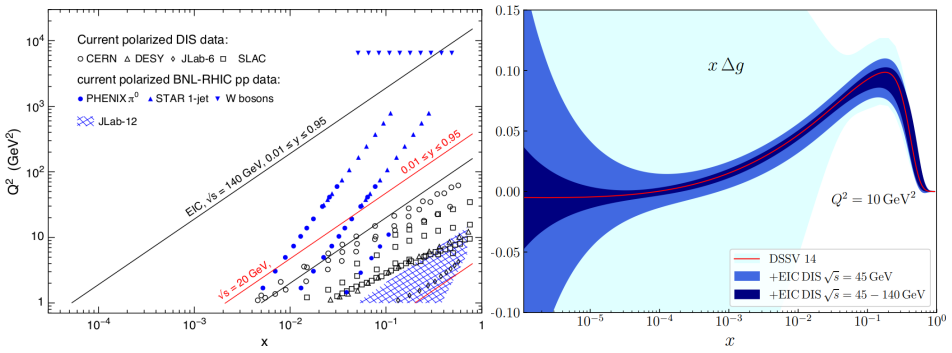

Fig. 6. Left: Comparison of the $x - Q^2$ coverage of the EIC at two different center-of-mass energies with polarized ep experiments conducted at CERN, DESY, Jefferson Lab, and SLAC, as well as pp experiments at RHIC. Source: [87]. Right: Impact of the projected EIC DIS pseudodata on the gluon helicity distribution. The figure displays the uncertainty bands resulting from the fit that includes the $\sqrt{s} = 44.7$ GeV DIS pseudodata and the reweighting with $\sqrt{s} = 141.4$ GeV pseudodata, in addition to the DSSV14 estimate [18]. Source: [86, 87].

Fragmentation functions provide valuable information on the struck parton, which can be used to improve the understanding of the nucleon's helicity structure. SIDIS measurements at the EIC that detect pions and kaons in addition to the scattered lepton will significantly enhance access to sea quark helicities compared to inclusive DIS measurements. Detailed studies using the PEPSI polarized Monte Carlo generator [88] and following the DSSV extractions [18, 19] show that the expected EIC measurements with polarized proton and ^{3}He beams at various collision energies could substantially reduce the uncertainties associated with all three sea-quark helicities [86]. As seen in Fig. 7, the reduction in the uncertainties of all three sea-quark helicities, $\Delta\bar{u}$, Δd, $\Delta\bar{s}$, is substantial compared to the current level of understanding. This reduction in uncertainties is particularly significant at low-x values for the highest collision energies, while intermediate- to higher-x values receive the biggest improvements already from the lower collision energies. In particular, the strange sea polarization's contribution to the spin sum rule can be conclusively determined at $x > 0.5 \times 10^{-5}$ by the EIC SIDIS data. Similar studies with pseudodata and reweighting techniques on the NNPDFpol replicas also indicate that similar improvements to the sea-quark helicities are achievable [20, 87, 89].

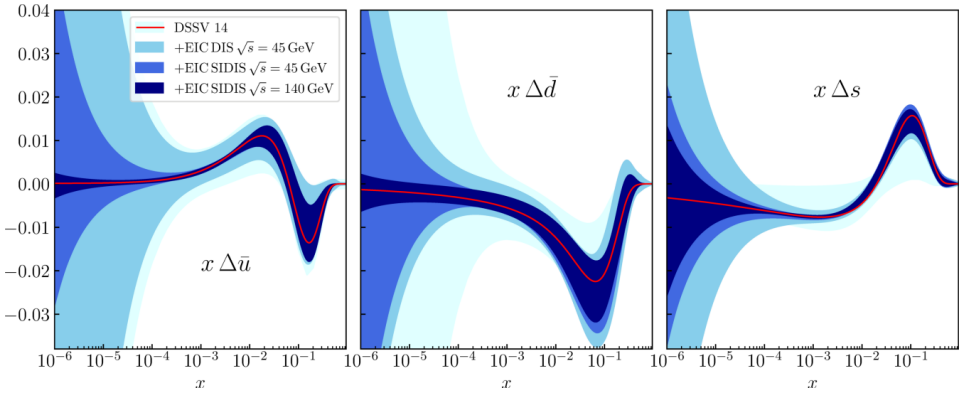

Fig. 7. The anticipated impact of the EIC SIDIS data on the distribution of helicity in sea quarks. The figure displays the uncertainty bands obtained from a fit that includes the pseudodata for at center-of-mass energy of $\sqrt{s} = 44.7$ GeV and from reweighting the SIDIS pseudo-data at $\sqrt{s} = 44.7$ and $\sqrt{s} = 141.4$ GeV. The DSSV14 estimate [18] is also plotted for comparison. Source: [86, 87].

4. Summary

The nucleon longitudinal spin structure has been extensively studied over decades using a variety of techniques, including Deep Inelastic Scattering, Semi-Inclusive Deep Inelastic Scattering, and proton–proton collisions. Polarized DIS cross-section asymmetries studied at SLAC, CERN, DESY, and JLab provide crucial information about the helicity structure of valence quarks inside nucleons. The complementary approach of studying longitudinal spin structure via strong interactions in pp collisions at RHIC provides access to gluons and the polarized quark sea. The complementarity of experiments utilizing both lepton scattering processes and hadron–hadron interactions is crucial in unraveling the complex nucleon spin structure. The upcoming EIC will provide a deep insight into the longitudinal spin structure of nucleons over a wide range of x and Q^2, which is critical to understanding the gluon and quark sea contributions to the nucleon spin.

The work is supported by the U.S. Department of Energy, Office of Science, Office of Nuclear Physics under contract No. DE-AC02-06CH11357. The author would like to thank the conveners of the STAR, PHENIX, and Hall C E12-06-110 collaborations for their valuable comments and feedback.

REFERENCES

[1] M.J. Alguard *et al.*, *Phys. Rev. Lett.* **41**, 70 (1978).
[2] G. Baum *et al.*, *Phys. Rev. Lett.* **51**, 1135 (1983).
[3] European Muon Collaboration (J. Ashman *et al.*), *Nucl. Phys. B* **328**, 1 (1989).
[4] Spin Muon Collaboration (B. Adeva *et al.*), *Phys. Rev. D* **58**, 112001 (1998).
[5] P.L. Anthony *et al.*, *Phys. Rev. D* **54**, 6620 (1996).
[6] E143 Collaboration (K. Abe *et al.*), *Phys. Rev. D* **58**, 112003 (1998).
[7] E154 Collaboration (K. Abe *et al.*), *Phys. Rev. Lett.* **79**, 26 (1997).
[8] P.L. Anthony *et al.*, *Phys. Lett. B* **463**, 339 (1999).
[9] E155 Collaboration (P.L Anthony *et al.*), *Phys. Lett. B* **493**, 19 (2000).
[10] HERMES Collaboration (K. Ackerstaff *et al.*), *Phys. Lett. B* **404**, 383 (1997).
[11] HERMES Collaboration (A. Airapetian *et al.*), *Phys. Rev. D* **75**, 012007 (2007).
[12] COMPASS Collaboration (M.G. Alekseev *et al.*), *Phys. Lett. B* **690**, 466 (2010).
[13] C. Adolph *et al.*, *Phys. Lett. B* **753**, 18 (2016).
[14] C. Adolph *et al.*, *Phys. Lett. B* **769**, 34 (2017).

[15] Jefferson Lab Hall A Collaboration (D.S. Parno *et al.*), *Phys. Lett. B* **744**, 309 (2015).

[16] CLAS Collaboration (Y. Prok *et al.*), *Phys. Rev. C* **90**, 025212 (2014).

[17] CLAS Collaboration (N. Guler *et al.*), *Phys. Rev. C* **92**, 055201 (2015).

[18] D. de Florian, R. Sassot, M. Stratmann, W. Vogelsang, *Phys. Rev. Lett.* **113**, 012001 (2014).

[19] D. de Florian *et al.*, *Phys. Rev. D* **100**, 114027 (2019).

[20] NNPDF Collaboration (E.R. Nocera *et al.*), *Nucl. Phys. B* **887**, 276 (2014).

[21] E. Leader, A.V. Sidorov, D.B. Stamenov, *Phys. Rev. D* **91**, 054017 (2015).

[22] Jefferson Lab Angular Momentum Collaboration (N. Sato *et al.*), *Phys. Rev. D* **93**, 074005 (2016).

[23] Jefferson Lab Angular Momentum Collaboration (J.J. Ethier, N. Sato, W. Melnitchouk), *Phys. Rev. Lett.* **119**, 132001 (2017).

[24] H. Khanpour, S. Taheri Monfared, S. Atashbar Tehrani, *Phys. Rev. D* **95**, 074006 (2017).

[25] A. Khorramian, E. Leader, D.B. Stamenov, A. Shabanpour, *Phys. Rev. D* **103**, 054003 (2021).

[26] C. Bourrely, J. Soffer, *Phys. Lett. B* **740**, 168 (2015).

[27] H.-W. Lin *et al.*, *Prog. Part. Nucl. Phys.* **100**, 107 (2018).

[28] M. Salimi-Amiri, A. Khorramian, H. Abdolmaleki, F.I. Olness, *Phys. Rev. D* **98**, 056020 (2018).

[29] D. de Florian, W. Vogelsang, *Phys. Rev. D* **99**, 054001 (2019).

[30] Spin Muon Collaboration (B. Adeva *et al.*), *Phys. Lett. B* **420**, 180 (1998).

[31] HERMES Collaboration (K. Ackerstaff *et al.*), *Phys. Lett. B* **464**, 123 (1999).

[32] HERMES Collaboration (A. Airapetian *et al.*), *Phys. Rev. D* **71**, 012003 (2005).

[33] COMPASS Collaboration (M. Alekseev *et al.*), *Phys. Lett. B* **660**, 458 (2008).

[34] COMPASS Collaboration (M. Alekseev *et al.*), *Phys. Lett. B* **680**, 217 (2009).

[35] COMPASS Collaboration (M.G. Alekseev *et al.*), *Phys. Lett. B* **693**, 227 (2010).

[36] HERMES Collaboration (A. Airapetian *et al.*), *Phys. Rev. D* **99**, 112001 (2019).

[37] PHENIX Collaboration (A. Adare *et al.*), *Phys. Rev. Lett.* **106**, 062001 (2011).

[38] STAR Collaboration (M.M. Aggarwal *et al.*), *Phys. Rev. Lett.* **106**, 062002 (2011).

[39] STAR Collaboration (L. Adamczyk *et al.*), *Phys. Rev. Lett.* **113**, 072301 (2014).

[40] PHENIX Collaboration (A. Adare *et al.*), *Phys. Rev. D* **93**, 051103 (2016).

[41] PHENIX Collaboration (A. Adare *et al.*), *Phys. Rev. D* **98**, 032007 (2018).
[42] STAR Collaboration (J. Adam *et al.*), *Phys. Rev. D* **99**, 051102 (2019).
[43] Jefferson Lab Angular Momentum Collaboration (C. Cocuzza, W. Melnitchouk, A. Metz, N. Sato), *Phys. Rev. D* **106**, L031502 (2022).
[44] STAR Collaboration (B.I. Abelev *et al.*), *Phys. Rev. Lett.* **97**, 252001 (2006).
[45] STAR Collaboration (B.I. Abelev *et al.*), *Phys. Rev. Lett.* **100**, 232003 (2008).
[46] STAR Collaboration (L. Adamczyk *et al.*), *Phys. Rev. D* **86**, 032006 (2012).
[47] STAR Collaboration (L. Adamczyk *et al.*), *Phys. Rev. Lett.* **115**, 092002 (2015).
[48] STAR Collaboration (J. Adam *et al.*), *Phys. Rev. D* **100**, 052005 (2019).
[49] STAR Collaboration (M.S. Abdallah *et al.*), *Phys. Rev. D* **103**, L091103 (2021).
[50] STAR Collaboration (M.S. Abdallah *et al.*), *Phys. Rev. D* **105**, 092011 (2022).
[51] STAR Collaboration (L. Adamczyk *et al.*), *Phys. Rev. D* **95**, 071103 (2017).
[52] STAR Collaboration (J. Adam *et al.*), *Phys. Rev. D* **98**, 032011 (2018).
[53] PHENIX Collaboration (A. Adare *et al.*), *Phys. Rev. D* **76**, 051106 (2007).
[54] PHENIX Collaboration (A. Adare *et al.*), *Phys. Rev. Lett.* **103**, 012003 (2009).
[55] PHENIX Collaboration (A. Adare *et al.*), *Phys. Rev. D* **79**, 012003 (2009).
[56] STAR Collaboration (B.I. Abelev *et al.*), *Phys. Rev. D* **80**, 111108 (2009).
[57] STAR Collaboration (L. Adamczyk *et al.*), *Phys. Rev. D* **89**, 012001 (2014).
[58] PHENIX Collaboration (A. Adare *et al.*), *Phys. Rev. D* **90**, 012007 (2014).
[59] PHENIX Collaboration (A. Adare *et al.*), *Phys. Rev. D* **93**, 011501 (2016).
[60] STAR Collaboration (J. Adam *et al.*), *Phys. Rev. D* **98**, 032013 (2018).
[61] PHENIX Collaboration (U.A. Acharya *et al.*), *Phys. Rev. D* **102**, 032001 (2020).
[62] PHENIX Collaboration (N.J. Abdulameer *et al.*), *Phys. Rev. Lett.* **130**, 251901 (2023).
[63] Jefferson Lab Angular Momentum Collaboration (Y. Zhou, N. Sato, W. Melnitchouk), *Phys. Rev. D* **105**, 074022 (2022).
[64] STAR Collaboration (J. Kwasizur), «Longitudinal Double-Spin Asymmetries for Dijet Production at Intermediate Pseudorapidity in Polarized Proton–Proton Collisions at , $\sqrt{s} = 510$ GeV», in: «APS Division of Nuclear Physics Meeting Abstracts», 2020, https://ui.adsabs.harvard.edu/abs/2020APS..DNP.DM009K
[65] N. Lukow, «Constraining the Polarized Gluon Distribution Function of the Proton with Recent STAR Measurements», in: «Proceedings of the 24$^{\text{th}}$ International Spin Symposium (SPIN2021)», 2021.
[66] STAR Collaboration (Z. Chang, T. Lin), arXiv:2306.11306 [hep-ex].

[67] PHENIX Collaboration (A. Adare *et al.*), *Phys. Rev. D* **93**, 051103 (2016).

[68] STAR Collaboration (J. Adam *et al.*), *Phys. Rev. D* **99**, 051102 (2019).

[69] E.-C. Aschenauer *et al.*, arXiv:2302.00605 [nucl-ex].

[70] A. Kolarkar *et al.*, «Hall C E12-06-110 Experiment Proposal: Measurement of Neutron Spin Asymmetry A_1^n in the Valence Quark Region Using an 11 GeV Beam and a Polarized ^{3}He Target in Hall C», 2006.

[71] S. Kuhn *et al.*, «Hall B E12-06-109 Experiment Proposal: The Longitudinal Spin Structure of the Nucleon», 2006.

[72] E12-06-110 Collaboration (W. Henry), «A Measurement of the Neutron Spin Structure at High-x in the 12 GeV Era», talk at the 2022 JLUO Annual Meeting, 2022.

[73] E12-06-110 Collaboration (M. Chen), «Precision Measurement of the Neutron Asymmetry A_1^n at Large Bjorken x at 12 GeV JLab», talk at the XXIX International Workshop on Deep-Inelastic Scattering and Related Subjects, Zenodo, November 2022.

[74] P.L. Anthony *et al.*, *Phys. Rev. D* **54**, 6620 (1996).

[75] E154 Collaboration (K. Abe *et al.*), *Phys. Rev. Lett.* **79**, 26 (1997).

[76] HERMES Collaboration (K. Ackerstaff *et al.*), *Phys. Lett. B* **404**, 383 (1997).

[77] Jefferson Lab Hall A Collaboration (X. Zheng *et al.*), *Phys. Rev. C* **70**, 065207 (2004).

[78] Jefferson Lab Hall A Collaboration (D.S. Parno *et al.*), *Phys. Lett. B* **744**, 309 (2015).

[79] Jefferson Lab Hall A Collaboration (D. Flay *et al.*), *Phys. Rev. D* **94**, 052003 (2016).

[80] N. Isgur, *Phys. Rev. D* **59**, 034013 (1999).

[81] C. Bourrely, J. Soffer, F. Buccella, *Eur. Phys. J. C* **23**, 487 (2002).

[82] I.C. Cloët, W. Bentz, A.W. Thomas, *Phys. Lett. B* **621**, 246 (2005).

[83] C.D. Roberts, R.J. Holt, S.M. Schmidt, *Phys. Lett. B* **727**, 249 (2013).

[84] E. Leader, A.V. Sidorov, D.B. Stamenov, *Int. J. Mod. Phys. A* **13**, 5573 (1998).

[85] H. Avakian, S.J. Brodsky, A. Deur, F. Yuan, *Phys. Rev. Lett.* **99**, 082001 (2007).

[86] I. Borsa *et al.*, *Phys. Rev. D* **102**, 094018 (2020).

[87] R. Abdul Khalek *et al.*, *Nucl. Phys. A* **1026**, 122447 (2022).

[88] L. Mankiewicz, A. Schäfer, M. Veltri, *Comput. Phys. Commun.* **71**, 305 (1992).

[89] E.R. Nocera, arXiv:1702.05077 [hep-ph].